

Integrated Cleat Analysis and Coal Quality on CBM Exploration at Sangatta II PSC, Kutai Basin, Indonesia*

Nita Apriyani¹, Suharmono¹, Muhammad Momen¹, Setiabudi Djaelani¹, Arifin Sodli¹, Andrean Satria², and Anom Seto Murtani²

Search and Discovery Article #80412 (2014)

Posted October 13, 2014

*Adapted from extended abstract prepared in conjunction with poster presentation at AAPG International Conference & Exhibition, Istanbul, Turkey, September 14-17, 2014, AAPG©2014

¹Energi Mega Persada, South Jakarta, DKI Jakarta, Indonesia (muhammed.momen@energi-mp.com)

²Schlumberger, Greater Jakarta Area, Indonesia

Abstract

This study was undertaken to determine cleat orientation, the relationship between cleat spacing, aperture, and cleat height, interpretation for cleat density, cleat volume and permeability for Balikpapan Fm. Miocene age coals. The methods used in this study includes fieldwork, quantitative analysis, fracture modeling using a Hybrid Model and laboratory analysis including proximate, maceral and Scanning Electron Microscope were conducted. The cleat orientation of the Balikpapan Formation measured at outcrop shows three main different domains cleat strike where the face cleat in Bengalon area has general E–W orientation, in North Pinang area has general NNW-SSE orientation and in the South Pinang area relative NE-SW. The largest variation of cleat direction between adjacent coalbed occurs where a large horizontal distance separates two sample locations. Face cleat with a NNW-SSE orientation were interpreted as the result of superimposed endogenic process, the process associated with coalification. Face cleat with N-E and NE-SW orientation are mainly associated with local tectonic stress. Cleat formation is influenced by mechanical in response to tectonic and geochemical processes related to coal composition. Higher calorific value and low ash content corresponded to high cleat densities. Higher total sulphur corresponded to lower cleat density. Perhaps total sulfur content has been affected by local environmental factors. Quantitative analysis of cleat and fracture data from this study indicate that a power-law distribution exists between cumulative cleats with spacing and aperture, fractal dimension (c) ranges from 0.79 to 2.06 and r-square values greater than 0.90. Coal quality was affected cleat intensity and attributes. The cleat density for individual seams varies between 0.17 cm/cm² and 0.51 cm/cm², cleat density increases toward Pinang Dome, related to structural position. Based on SEM photos, outcrop sample cleat apertures range from 0.8 µm to 15 µm, increasing to 15 µm to 30 µm in the direction of maximum stress. Core samples apertures ranged from 0.1 µm to 6 µm and filling by pyrite. Characterisation of cleat attributes allows an indirect estimation of permeability, which are critical parameters for commercial CBM development. Permeability was much higher in outcrops (200–5000 md) than in core samples from 260 m depth (0.1-19 md).

Introduction

In CBM plays, coal is both source rock and reservoir rock. Coal commonly has porosity but very low matrix permeability, so fractures are needed for commercial rates of gas to flow from the matrix (coal macerals) micropores and microscopic laminations to the producing wells.

Cleats are natural fractures that form in coal seams as the result of coal dehydration, local and regional stresses, and unloading of overburden. Cleats usually occur in two sets, Face Cleats and Butt Cleats that are, in most instances, mutually perpendicular and perpendicular to the bedding plane (Laubach et al., 1997). Face cleats are through-going cleats formed first, and are dominant, continuous and laterally extensive. Butt cleats end at Face Cleats, and are formed later (Laubach and Tremain, 1991). Face cleats form parallel to the direction of maximum compressive stress and perpendicular to the fold axis, whereas Butt Cleats are strain release fractures that form parallel to the fold axis (CSG, 2012). Understanding cleat geometry and orientation are important for CBM these are the pathways for gas to flow from the matrix to the wellbore.

Ammosov and Eremin (1963; in Ryan, 2002) used a genetic classification, that indicated that endogenetic fractures are the classic ‘cleats’ that form under tension probably in response to dewatering and shrinkage of the coal matrix as coal rank increases. On the other hand, exogenetic fractures are formed by regional stress fields and their orientations are controlled by these fields, so they are not necessarily perpendicular to coal seams. They can cut into other lithologic series.

Cleat spacing is related to rank, bed thickness, maceral composition and ash content. Cleat development is also influenced by lithotypes; dull lithotypes (inertinite rich layers) tend to be massive and poorly cleated whereas bright lithotypes (vitrain rich layers) are often finely banded and well cleated (Ryan, 2002). Cleats are generally more tightly spaced with increasing coal rank. Average cleat spacing in sub-bituminous coal is 2-15 cm, in high volatile bituminous coal is 0.3-2 cm, and in medium to high volatile bituminous coal is <1 cm (Cardott, 2001 (in CSG, 2012)). Therefore, cleat spacing is tighter in vitrinite-rich and low-ash coals, and in thin coal seams.

Cleats can be filled by secondary macerals especially in the low rank coal. Cleats can anneal in high rank coal such that they cannot be observed on the macro or micro scale (Xianbo Su et al., 2001). Cleat annealing is different process from cleat mineralization. Cleat annealing gradations are extensive, slight and partial (Yang and Han, 1979; Levine, 1993; Laubach et al., 1998). Xianbo Su et al., 2001 investigated two mechanism of cleat annealing: secondary maceral filling and agglutination.

Secondary maceral filling occurs commonly in low rank coals (brown coal and sub-bituminous coal), exudinite as secondary maceral fills cleats, bedding-plane fractures and occasionally empty lumens (Stach et al., 1982; Han, 1996; Chen et al., 1995). Cleat annealing begins at the initial stage of its formation ($R_{o,max}=0.3-0.6\%$). Agglutination means cleat walls fuse together under high temperature and pressure. When the cleat is formed, coal near the cleat wall will become thermoplastic as the consequence of progressive temperature and pressure increase as fluids in the cleat transfer heat and pressure (Henan Company of Coal Geology, 1991; in Xianbo Su et al., 2001). This paper discusses cleat characteristics and their relationship with coal rank, lithotypes including maceral composition and ash content, and cleat annealing. The aim is to predict coal permeability, which governs CBM production rates.

Regional Geology

The Sangatta II CBM PSC is located in the north part of the Kutai Basin, a tertiary sedimentary basin in East Kalimantan. The basin is bounded to the north by the Mangkalihat High. It hinges on the south to the Adang flexure (Adang Fault Zone). To the west, it is terminated by the Kuching High in the Kalimantan Central Ranges. To the east, it is open to the Strait of Makassar. The coals lay across one of several structural

culminations along the crest of a strongly asymmetrical anticline, which extends over 100 km in a NNE-SSW direction, where the Upper-Middle Miocene Balikpapan Formation is exposed at the surface as seen in [Figure 1](#).

Stratigraphy and Depositional Environment

Tertiary sediments in the East Kutai basin are very thick with different depositional facies. Sediment layers shows transgressive and regressive sequences like other basins in the west of Indonesia (Schlumberger, 1986). Regressive sequences in the Kutai Basin contain deltaic clastic layers until paralic, which are filled with coal beds until lignite, which created a deltaic complex environment containing deltaic deposition cycles. Every cycle began with delta plain deposits consisting with swamp deposits, channel deposits, point bars, natural levees, and crevasse splays. Delta front and pro-delta sediments were deposited in deeper waters. Then transgression deposited upper delta plain sediments followed by regression that deposited delta plain, upper delta front and pro-delta deposits. These deltaic cycles can be shown in prograding Kutai Basin, which have Eocene Epoch until Early Tertiary Epoch from West to East, marked by deposition of the Pamaluan Formation, Bebulu Formation (Early Miocene-Middle Miocene), Pulau Balang Formation, Balikpapan Formation (Middle Miocene), Kampung Baru Formation (Late Miocene – Pliocene), deltaic Mahakam deposits, which is Quaternary deposits. Generally, stratigraphy from younger to older is alluvial deposits, Kampung Baru Formation, Balikpapan Formation, and Pulau Balang Formation ([Figure 2](#)).

Tectonic Setting

Basement under the Lower Kutai Basin is interpreted to be continental in character and is typed as rafted transitional. The lower Kutai basement docked with earlier rafted basement segments in the Late Cretaceous to Palaeocene (70-60 Ma). The suture zone between this latest of rafted segments is the boundary between the Upper and Lower Kutai Basin. The suture zone trends NE in the northern portion of the basin, parallel to the Meratus Ophiolite Complex to the south. NW-SE trending Adang-Paternoster and Mangkalihat Fault Zones controlled the north and south of the Kutai Basin boundaries area. This zone is separated the relatively shallow area of the Barito and Mangkalihat Platforms in the south and north to the deeper part of the Kutai Basin. Farther northward, the Kutai Basin is separated from the Tarakan Basin by the Mangkalihat Ridge/Platform.

The onshore portion of the Mahakam Delta overlies a series tightly folded anticlines and broad synclines known collectively as the Samarinda Anticlinorium, which resulted from inversion of the Palaeogene basin (Chambers and Daley, 1995). Offshore Mahakam Delta area shows at least two phases of deformation. Middle Miocene and older rocks exhibit compressional folding and thrusting, while the over-lying Upper Miocene-Pliocene strata are only affected by extensional faulting (Malecek et al., 1993).

Methodology

Cleat mapping and coal sampling was performed on outcrops and from cores 260m deep. Measurements included coal position, thickness, bedding (strike/dip), description and stratigraphic section (MS). Outcrop scanline measurements included cleat orientation, type, aperture, height, spacing, and azimuth/plunge. Scanline length was set to coal thickness with a minimum of 5 metres. Window scans identified cleat orientation, type, aperture, intensity in an observation area of 1m x 1m. Coals samples underwent proximate analysis, ultimate analysis and

SEM (Scanning Electron Microscope). Quantitative analysis determined the relationship between cleat properties: cleat orientation, density, and aperture. Cleat origin was identified by rotation of cleats and bedding planes to the horizontal position. Permeability was estimated from an equation from Lucia (1983) and Scott (1999), which relates permeability to coal quality such as ash content, total sulphur, and moisture.

Cleat Orientation

Outcrop cleat measurements in coal seams of the Balikpapan Formation were taken in seventeen locations; fifteen in the Pinang area and two in the Bengal area. The locations stretched over 25 km. Some were near fault zones and folds, some were close to the dome, and some were in areas not affected by local structure. The number of cleat measurements at each station varied from 300 to 500 depending on coal thickness, coal characteristics and local geological structure.

Three main different cleat strike directions were seen:

- 1) South Pinang Area. The four locations were BE, E2, PM and MU. BE face cleat orientation was N 211° E and butt cleat orientation was N 120° E. E2 station cleats were in a fault zone and cleat orientation slightly differed from the general pattern in South Pinang, with face cleat orientation at N 239° E and butt cleat orientation at N 340° E. The PM and NU stations had face cleat orientation at N 34° E and butt cleat orientation at N 115° E.
- 2) North Pinang Area. The eleven locations were K19LR, B2, SU, MD, P4, OX, KL, K13, KJ, K12 and PY. Cleat orientation was influenced by the Pinang Dome. Face cleats were oriented northwest-southeast and butt cleats were oriented northeast-southwest. Orientation of face cleat varied between N 142° E to N 172° E and N 301° E to N 349° E, while butt cleat orientation varied between N 60° E to N 69° E and N 201° E to N 271° E.
- 3) Bengal area. The two locations were A and E. Face cleats were oriented west-east and butt cleats were oriented northwest-southeast. A face cleats were oriented N 81° E and butt cleats were oriented N 350° E. E face cleats were oriented N 105° E and no butt cleats were seen. Local geological structure may have affected cleat formation.

Summaries of cleat measurement and cleat orientation are shown in [Table 1](#) and [Figure 3](#).

Cleat Rotation

Cleats can be endogenic or exogenic. Endogenic cleats are formed due to changes in the properties of coal (coalification) associated with changes in the internal stress system, compaction and desiccation. Exogenic cleats are formed as result of the external stresses acting on the coal seam including tectonic stress, fluid pressure changes, folding and development of tensile stresses. Exogenic cleats typically have lower permeability. Endogenic cleats are angled 70°-90° to the bedding plane. Exogenic cleats are angled less than 70° to the bedding plane. Bedding and cleat data was rotated to the horizontal to represent initial deposition. [Figure 4](#) shows that most cleats were endogenic, except in A station (Bengal area) and BE station (South Pinang) where cleat angles were 51°-66°, possibly influenced by local stresses.

Quantitative Analysis

Scan-line and Window-scan measurements at fourteen locations measured cleat density, spacing, aperture, and height. Scan-line length followed coal thickness (0.12 m to 12 m) with a minimum length of 5 metres, resulting in 74 to 351 data points per location. Cleat length was not measured, as we could not see into the coal.

[Table 2](#) and [Figure 5](#) show that cleat density (total cleat height per area observed) ranged from 0.04 cm/cm² to 0.367 cm/cm². Average spacing ranged from 1.6 cm to 21.6 cm. Average apertures ranged from 0.02 cm to 0.15 cm. Average height ranged from 13 cm to 69 cm.

Cleat density increased near fault or fold zones. Average aperture in exogenic cleats was relatively small. [Figure 6](#) plots average density and spacing, and the relation between the two follows a power-law:

$$Y = 0.42X^{-0.78}$$

where Y is spacing (cm) and X is average density (cm/cm²). The correlation coefficient (R²) is 0.82.

[Figure 7](#) plots cleat density and cleat height, and the relation between the two follows an exponential distribution:

$$Y = 0.034e^{0.031X}$$

where, Y is average density (cm/cm²) and X is average height (cm). The correlation coefficient (R²) is 0.8.

Window scans measured face and butt cleat data on a 1m x 1m area at fourteen locations, resulting in 43 to 489 data points per location.

[Table 3](#) and [Figure 8](#) show that cleat density ranged from 0.17 cm/cm² to 0.5 cm/cm². Average aperture ranged from 0.02 cm to 0.06 cm. Average height ranged from 10.89 cm to 87.56 cm.

Cumulative-frequency fracture-size distributions provide a measure of fracture intensity (or average spacing) that explicitly accounts for fracture size and permits a comparison of data collected at different locations and/or observation scales (Ortega et al., 2006). The cumulative distribution of cleat spacing for each scanline was generated by sorting measurements of aperture and spacing from largest to smallest, and then normalising the data by registering the number of cleats in the range of a particular space or aperture in each analysis.

Cumulative fractures are related to spacing and aperture by the power-law:

$$f = be^{-c}$$

where f is cumulative number, b is cleat intensity, e is spacing, and c is a constant.

[Table 4](#) shows R^2 at each location ranged from 0.93-0.98. [Figure 9](#) and [Figure 10](#) show examples of the fit of the power law. [Table 5](#) shows cleat density from window scan analysis in the Pinang and Bengal area ranged from 0.17 cm/cm² to 0.51 cm/cm². [Figure 11](#) shows cleat density increases towards the Pinang Dome.

Coal Quality Analysis

Coal varied from brown to black. Black coal was shiny, composed of vitrain (laminated, very shiny, fractional konkoidal with vitrinite maceral rich, derived from wood and wood fibre) and clarain (thin laminated, partly shiny and dull with vitrinite maceral and liptinite rich, derived from spores, cuticles, pollen, sap). Low rank coal was more weathered than black coal. Thin layers of sandstone and mudstone with thickness varying from a few millimeters to a few centimetres ran through the coals. Coal quality was obtained from chemical analysis of coal samples in the laboratory, including proximate and ultimate analysis. Proximate analysis was performed to determine the amount of moisture, volatile matter, fixed carbon and ash. Ultimate analysis was performed to determine the chemical elements in coal such as carbon, hydrogen, oxygen, nitrogen, sulphur, additional elements and rare elements as seen in [Table 6](#).

Coal samples were collected at two locations along the horizontal scanline for proximate analysis. The results were integrated with quantitative analysis of scanline data. Quantitative data provided cleat density information at 20 cm intervals along the scanlines. Coal quality data was integrated to know the relationship between density and ash content, calorific value, fixed carbon, and total and average spacing of the ash content ([Figure 12](#)). Coal samples from the BE and E locations had higher calorific value and low ash content, and had higher cleat densities. Higher fixed carbon content corresponded to high cleat density. Total sulfur content had no clear relationship to cleat density. Higher total sulphur at location E corresponded to lower cleat density. At location BE, the opposite was true. Perhaps total sulfur content has been affected by local environmental factors.

Micro-Cleat Analysis

Micro-cleat analysis was conducted on outcrop samples and cores from 260 m depth with a scanning electron microscope (SEM) as seen in [Figure 13](#). Outcrop samples apertures ranged from 0.8 µm to 15 µm and increased in the maximum local stress direction to 15 µm to 30 µm. Face micro-cleats were better developed with larger apertures than butt micro-cleats. Micro-cleats were rarely filled by pyrite. Cleat agglutination was seen in coal with high density, with cleats entirely or partially annealed. Agglutination usually occurs in high rank coal because of the higher temperatures and pressures (X. Su et al., 2001). Core sample apertures ranged from 0.1 µm to 6 µm with a maximum of 30 µm.

Permeability Analysis

Permeability often governs the commerciality of CBM development. In CBM, almost all gas and water flow occurs in fractures and cleats. Permeability depends on cleat density, aperture and connectivity, and ranges from micro-Darcys to Darcys (Scott, 1999). Permeability can be

estimated from cleat attributes using the equations of Scott (1999), Lucia (1983) or Aguilera (1995). Lucia (1983) conducted a study of fractured carbonates that yielded a relationship between permeability, abundance of fractures, and fracture aperture:

$$K = (84.4 \times 10^5) W^3 / Z$$

where k is permeability (Darcys), w is fracture aperture (cm), and z is fracture spacing (cm). Aguilera (1995) combined this relation with Darcy's law:

$$\begin{aligned} k_f &= 8.35 \times 10^6 W^2 \\ \text{cubes, } k_2 &= (2/3) (K_f W^2 / Z) \\ \text{Match sticks, } k_2 &= (1/2) (k_f W^2 / Z) \end{aligned}$$

Input of Sangatta outcrop cleat data into this equation gives permeability ranging from 50 to 5,000 md as seen in [Table 7](#). Permeability increases towards the Pinang Dome as seen in [Figure 14](#). Micro-cleat data from core samples at 260 m showed a cleat density of 3-28 cleats per inch and apertures of 1 μm to 6 μm . Using the logarithmic graphic relationship (Lucia, 1983, and Scott, 2002), permeability ranges from 0.1 to 19 md as seen in [Figure 15](#).

Cleat Modeling

Data availability for this study consists of thirty 2D seismic lines (depth domain), twenty-six boreholes mining (BE seam), and field cleat measurement from one station. Two horizons interpreted for this particular study are Balikpapan Fm and Pulau Balang Fm. The structural model is built without accommodating faults since we are only interested to model the distribution of the cleats from BE seam. The four horizons used are near the top of the Balikpapan Formation, the top of Coal Seam BE, the base of Coal Seam BE, and the top of the Pulau Balang Formation. The grid size is 100x100 m with a total number of cells of 82,308.

Fracture driver is a property in the entire grid that could give us some additional info on the lateral spatial extent of fractures. It works as a guide for the 3D distribution of cleat Intensity. There are five attributes used: curvature, edge detection, influential surface data, depth correction, and structural position. Fractures are normally related to faults and fold (syncline and anticline), either as intense fracturing in localized zones (corridors), or as conjugate fracture sets around a fault (main fractures parallel to fault direction and a smaller fracture set at approx 65° to the main fractures). We assumed that, structurally, the intensity of cleats should be divided into four regions, which are moderate flank is 0.18; steep flank is 0.19; fault is 0.23; and syncline is 0.10 (Prasongko et al., 2007).

The above five attributes are combined using a Neural Network method to produce one driver attribute to cleat distribution guide ([Figure 16](#)). Petrel combines two approaches to standard fracture modeling by the use of a hybrid model that consists of discrete fracture network - (DFN) where the large/important fractures are modeled explicitly as discrete patches and implicit fracture model - (IFM) where the residual part of the distribution (smaller fractures) is statistically represented as grid properties. The parameter of fracture network modeling is as follows:

distribution, fracture geometry, orientation, regional trends and aperture. Based on cleat network model, cleat distribution on BE seam in Sangatta field decreased toward the increasing depth as shown on [Figure 16](#).

Conclusions

- Face cleat orientation in the Balikpapan Formation follows three trends; E-W in the Bengalon area, NNW-SSE in the North Pinang area and NE-SW in the South Pinang area. NNW-SSE orientation was interpreted as the result of endogenic process associated with coalification. N-E and NE-SW orientation is associated with local tectonic stresses. Wells should be placed perpendicular to the face cleat orientation.
- Cleat formation is influenced by mechanical and geochemical processes related to coal composition, where different process may occur from initial cleat formation until now.
- Characterization of cleat distributions and orientation provides a tool to indirectly estimate porosity and permeability in coal reservoirs, which are critical parameters for commercial CBM development.
- Quantitative analysis of cleat attributes indicate a power law relationship between cleat density and spacing, an exponential law relationship between cleat density and height, and a power law relationships between cumulative fractures with spacing and aperture, with a goodness of fit of around 0.93.
- Cleat density for individual seams varies between 0.17 cm^{-1} and 0.51 cm^{-1} . Density increases towards the Pinang Dome and is related to local structural position.
- Based on SEM photos, outcrop sample cleat apertures range from $0.8 \text{ }\mu\text{m}$ to $15 \text{ }\mu\text{m}$, increasing to $15 \text{ }\mu\text{m}$ to $30 \text{ }\mu\text{m}$ in the direction of maximum stress. Core samples apertures ranged from $0.1 \text{ }\mu\text{m}$ to $6 \text{ }\mu\text{m}$.
- Characterisation of cleat attributes allows an indirect estimation of permeability. Permeability was much higher in outcrops (200-5,000 md) than in core samples from 260 m depth (0.1 to 19 md).

Selected References

Ammosov, L.L., and L.V. Eremin, 1963, Fracturing in coal: Translated from Russian by the Israel Program for Russian Translations, 1963.

Chambers, J.L.C., and T. Daley, 1995, A tectonic model for the onshore Kutai Basin, East Kalimantan, based on an integrated geological and geophysical interpretation: Indonesian Petroleum Association, Proceedings 24th Annual Convention, Jakarta 1995, v. I, p. 111-130.

Chen, G., and S. Harpalani, 1995, Study of fracture network in coal: in Myer, L.R., Cook, N.G.W., Goodman, R.E., Tsang, C.-F. Eds., Fractured and Jointed Rock Masses. Balkema, Rotterdam, p. 431–434.

Laubach, S.E., R.A. Marret, J.E. Olson, and A.R. Scott, 1998, Characteristics and Origin of Coal Cleat: a review: International Journal of Coal Geology, v. 35, p. 175-207.

Laubach, S.E., and C.M. Tremain, 1991, Regional Coal Fracture Patterns And Coalbed Methane Development: The 32nd U.S. Symposium on Rock Mechanics (USRMS), 10-12 July, Norman, Oklahoma.

Levine, J.R., 1993, Coalification: The evolution of coal as source rock and reservoir rock for oil and gas: in Law, B.E., Rice, D.D. Eds., Hydrocarbons from Coal, V. 38, AAPG Studies in Geology, p. 39–78.

Lucia, F.J., 1983. Petrophysical parameters estimated from visual description of carbonate rocks: a field classification of carbonate pore space: Journal of Petroleum Technology, p. 626-637, DOI <http://dx.doi.org/10.2118/10073-PA>.

Malecek, S.J., C.M. Reaves, and W.S. Atmadja, 1993, Seismic stratigraphy of Miocene and Pliocene age outer shelf and slope sedimentation in the Makassar PSC, Offshore Kutei Basin: in Proceedings Indonesian Petroleum Association, 22nd Annual Convention, p. 345–371.

Ortega, J.O., R.A. Marrett, and S.E. Laubach, 2006, A Scale Independent Approach to Fracture Intensity and Average Spacing Measurements: AAPG Bulletin, v. 90/2, p. 193-208.

Prasongko, K.B., N. Sudarto, and K. Anggayana, 2007, Karakteristik Cleat pada Lapisan Batubara yang Terlipat dan Tersesarkan di Daerah Palaran dan Busui, Kalimantan Timur: Journal Geoaplika, v. 2/2, p. 53-66.

Ryan, B., 2002, Cleat Development in Some British Columbia Coal: Geol. Fieldwork 2002 165-183 (2003), paper 2003-1. Web accessed September 28, 2014. <http://www2.gov.bc.ca/gov/DownloadAsset?assetId=66CC6F78BC2E4153B0334E0AD3B61123>.

Stach, E., M.T.H. Mackowsky, M. Teichmueller, G.H. Taylor, and D.R. Chandra, 1982, Coal Petrology: Gebruder Borntraeger, Stuttgart–Berlin, p. 5–86.

Su, X., Y. Feng, J. Chen, and J. Pan, 2001, The Characteristics and Origin of Cleats in Coal from Western North China: International Journal of Coal Geology, v. 47, p. 51-62.

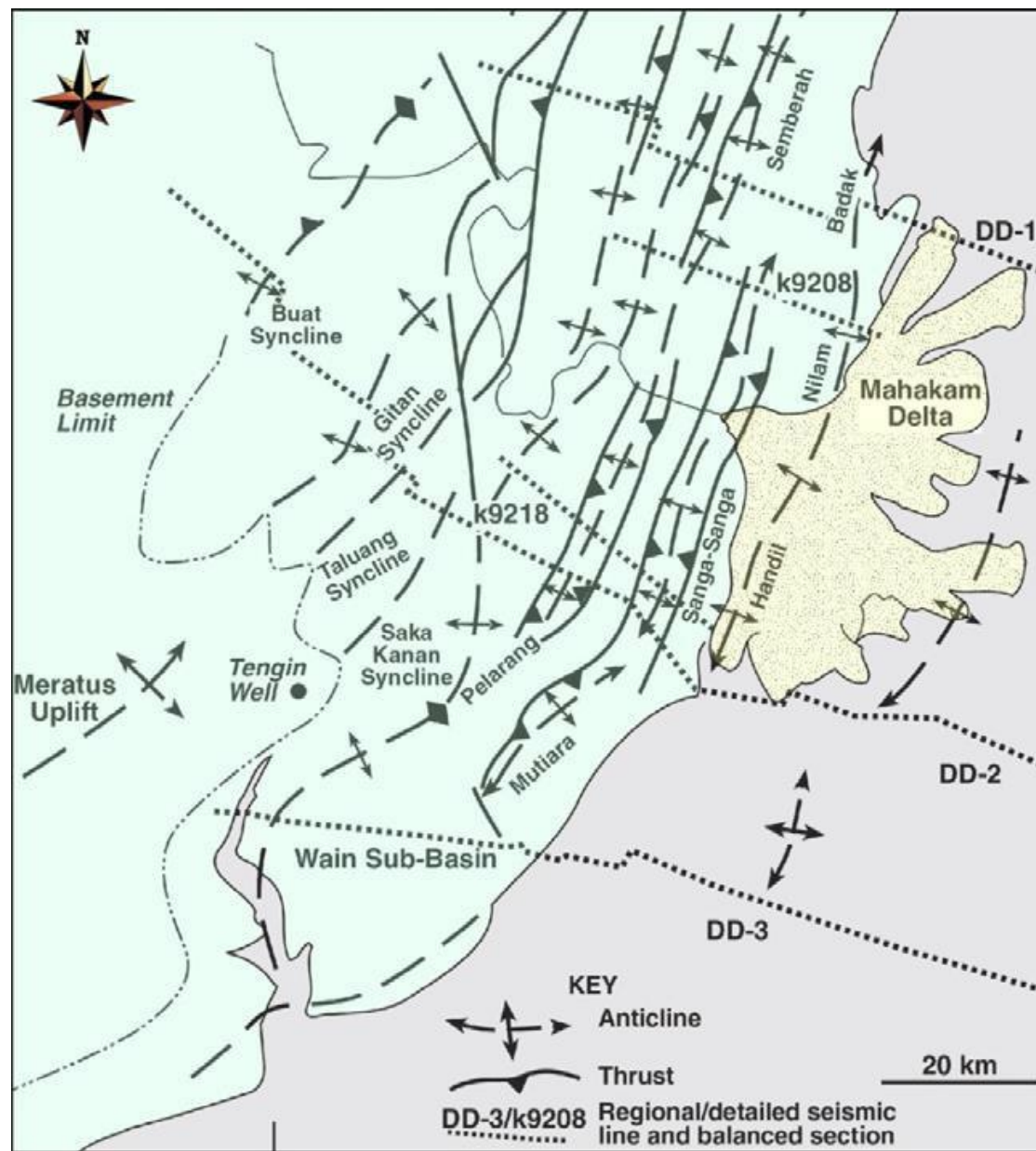


Figure 1. Structural geology of Kutai Basin.


MASA ERA	ZAMAN PERIOD	KALA EPOCH	ENDAPAN PERMUKAAN SURFICIAL DEPOSITS	BATUAN SEDIMEN SEDIMENTARY ROCKS	DESKRIPSI	
KENOZOIKUM CENOZOIC	KUARTER QUATERNARY	HOLOSEN HOLOCENE	<div>Qa</div>		Endapan Alluvial Qa: Material lepas berukuran lempung hingga pasir halus dan material organik. Lingkungan pengendapan fluvial-lacustrine	
		PLEISTOSEN PLEISTOCENE			Formasi Kampungbaru Tpkb: Batupasir kuarsa yang bersifat lepas dengan sisipan batulempung, serpih, batulanau, dan lignit. Lingkungan pengendapan delta	
	KUARTER QUATERNARY	PLIOSEN PLIOCENE		<div>Tpkb</div>	Formasi Balikpapan Tmbp: Batupasir kuarsa dan batulempung dengan sisipan batulanau, serpih dan batubara. Lingkungan pengendapan delta	
		MIOSEN MIOCENE		AKHIR LATE	<div><div>Tmpb</div><div>Tmbp</div></div>	Formasi Pulau Balang Tmbp: Batupasir (greywacke), batupasir kuarsa, batugamping, batulempung dengan sisipan batubara. Lingkungan pengendapan darat-laut dangkal
				TENGAH MIDDLE		
				AWAL EARLY		
		OLIGOSEN OLIGOCENE		<div><div>Tomp</div><div>Tmb</div></div>		

Figure 2. Stratigraphy of Kutai Basin.

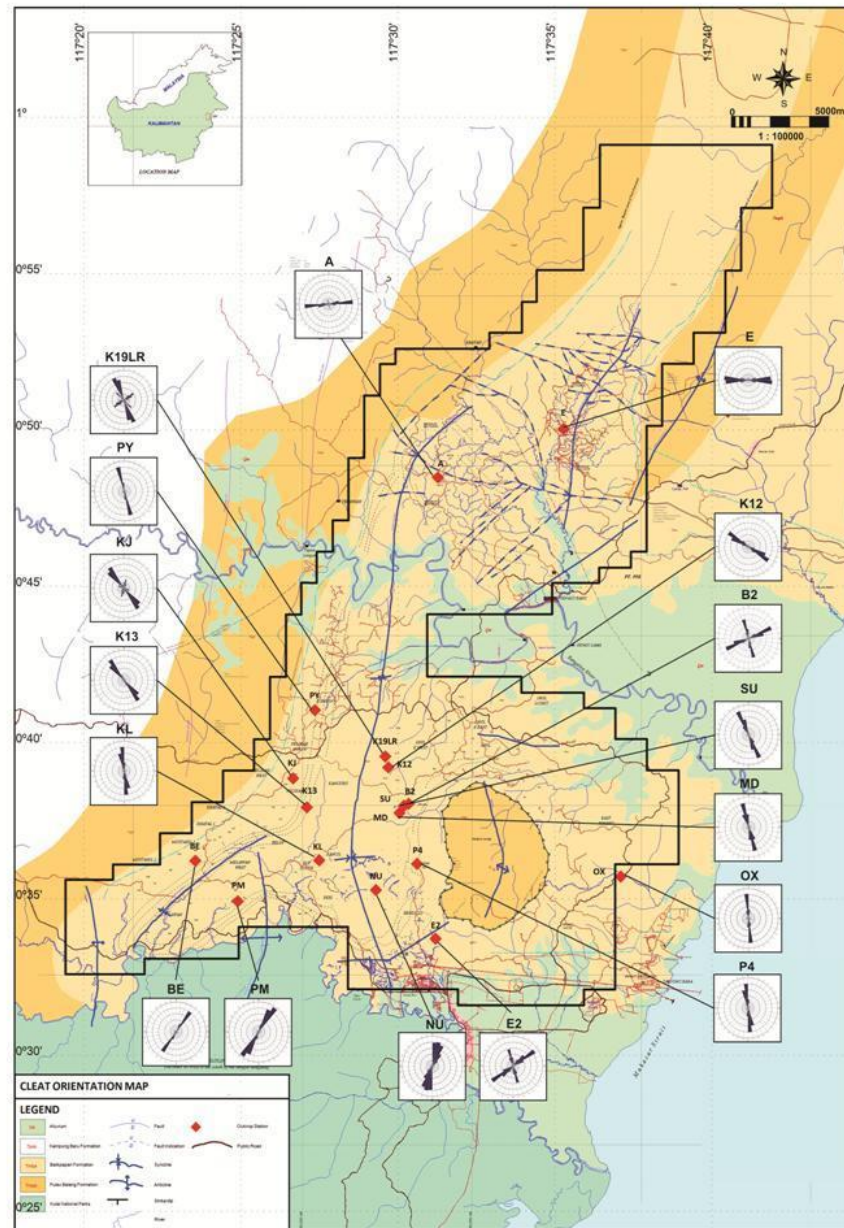


Figure 3. Cleat orientation map.

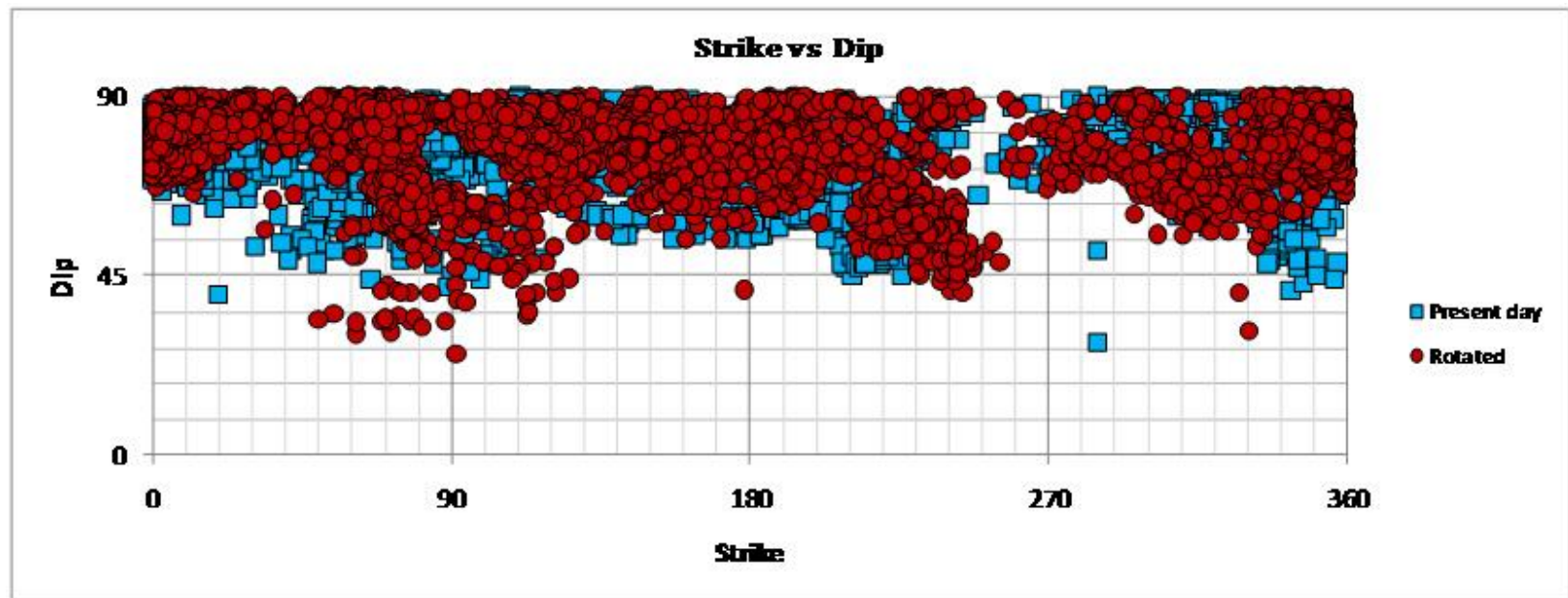


Figure 4. Strike vs. dip present-day cleats and rotated cleats.

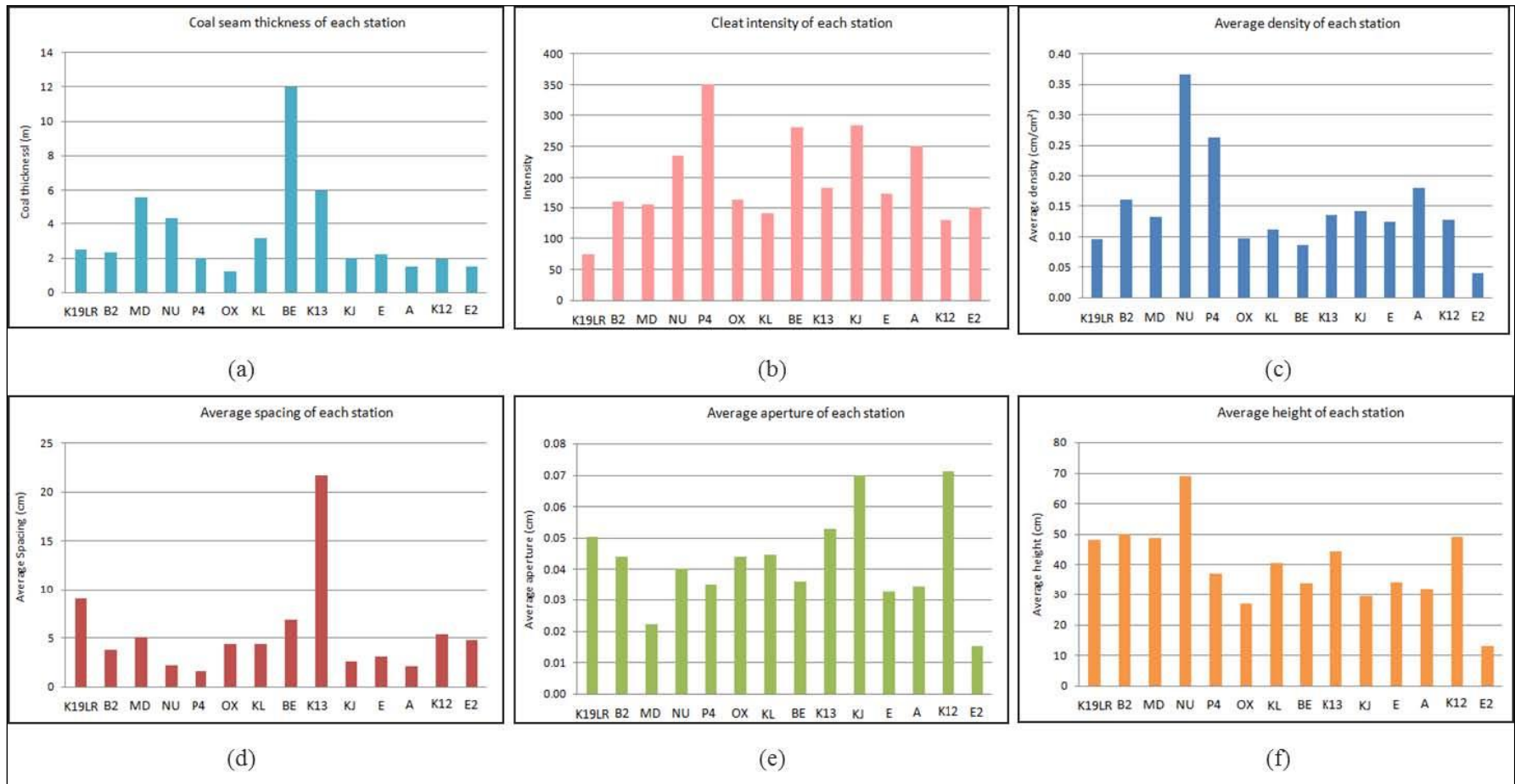


Figure 5. (a) Coal thickness on each station, (b) cleat intensity of scanline of each station, (c) average density of scanline on each station, (d) average spacing of scanline on each station, (e) average aperture of scanline on each station, (f) average height of scanline on each station.

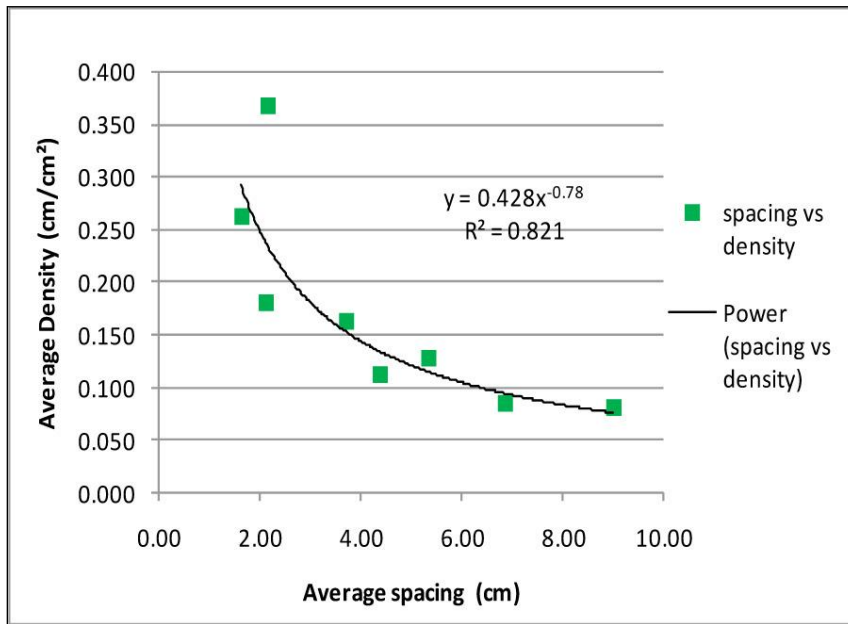


Figure 6. Average density and spacing.

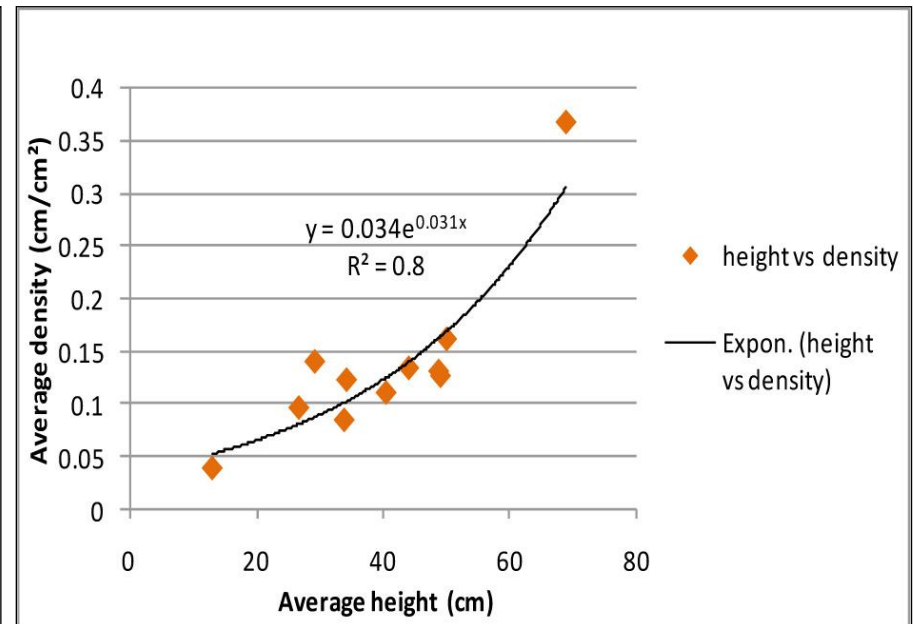


Figure 7. Average density and height.

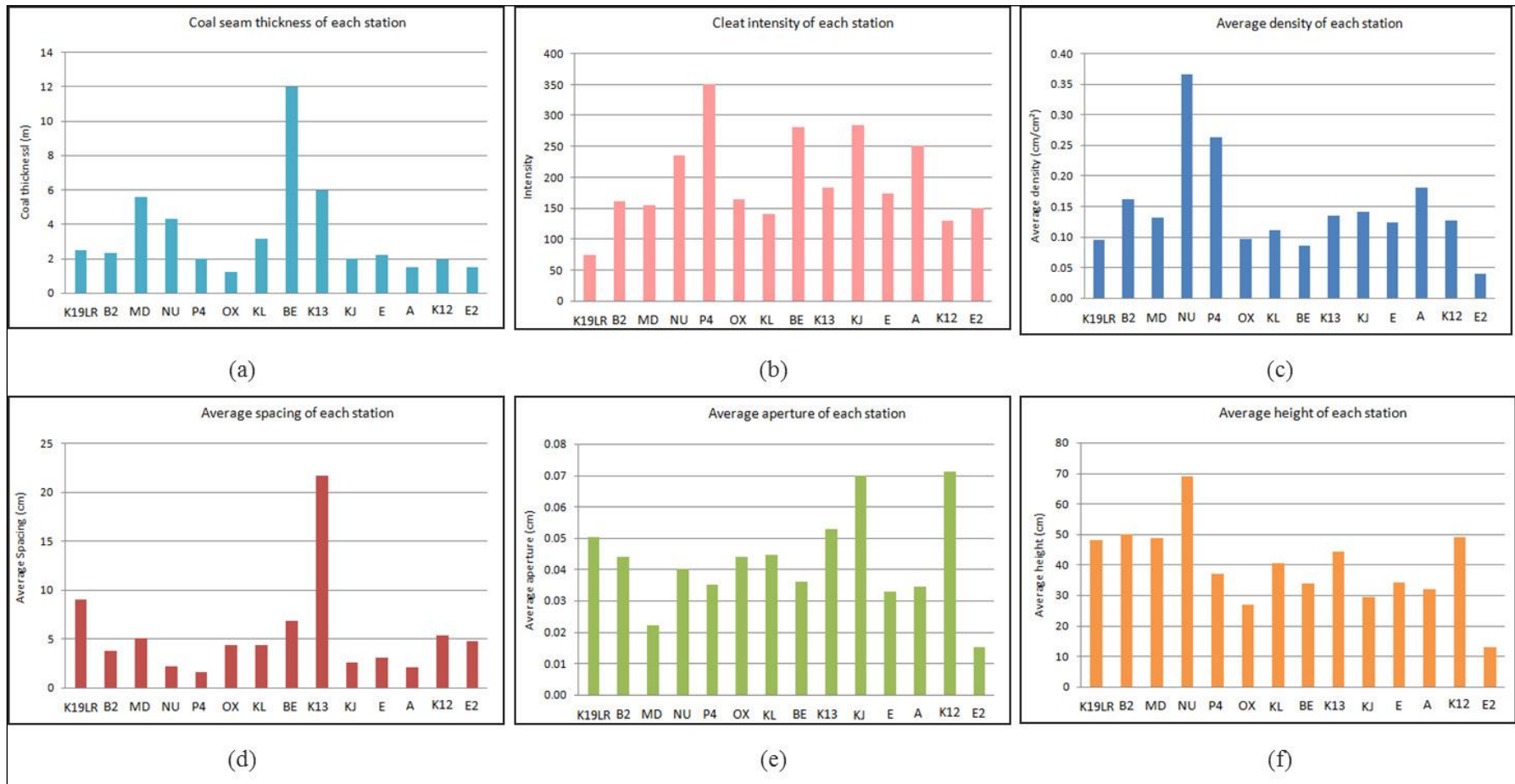


Figure 8. (a) Cleat intensity, (b) average density, (c) average aperture, (d) average height of window scan.

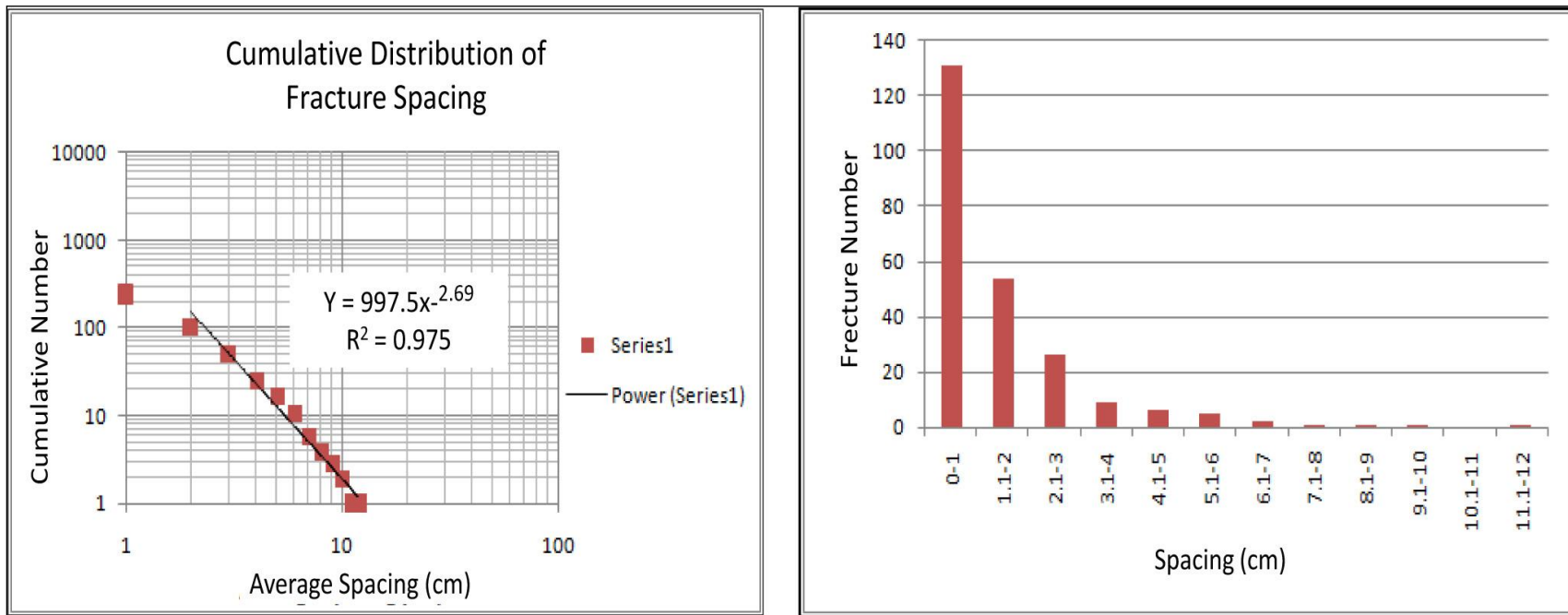


Figure 9. Cumulative distribution of fracture spacing.

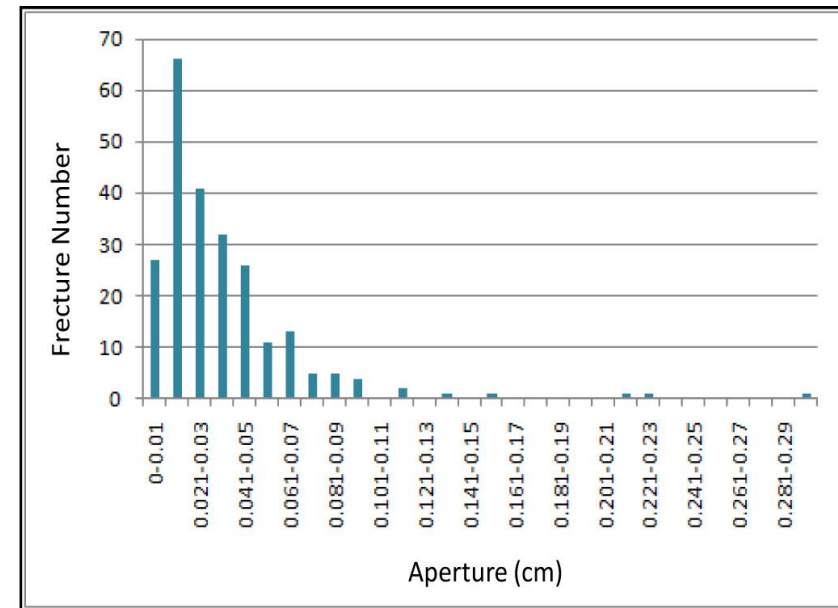
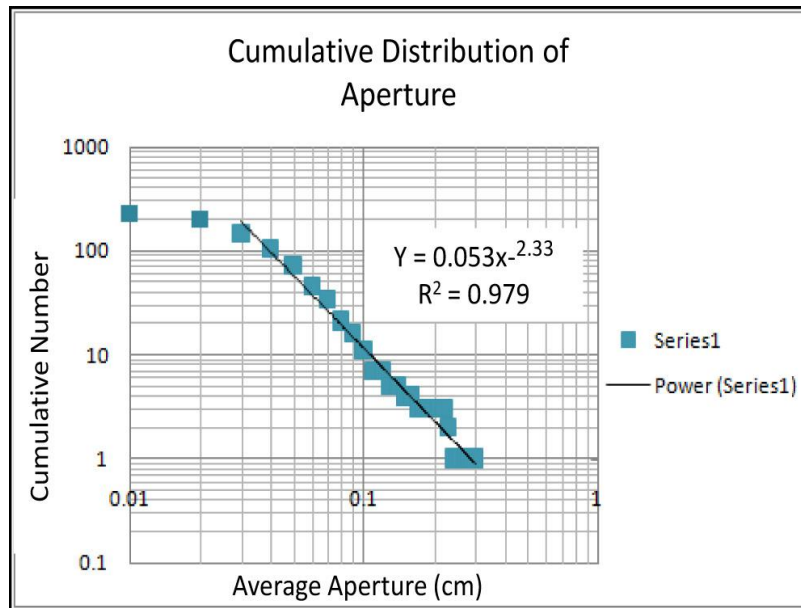


Figure 10. Cumulative distribution of aperture.

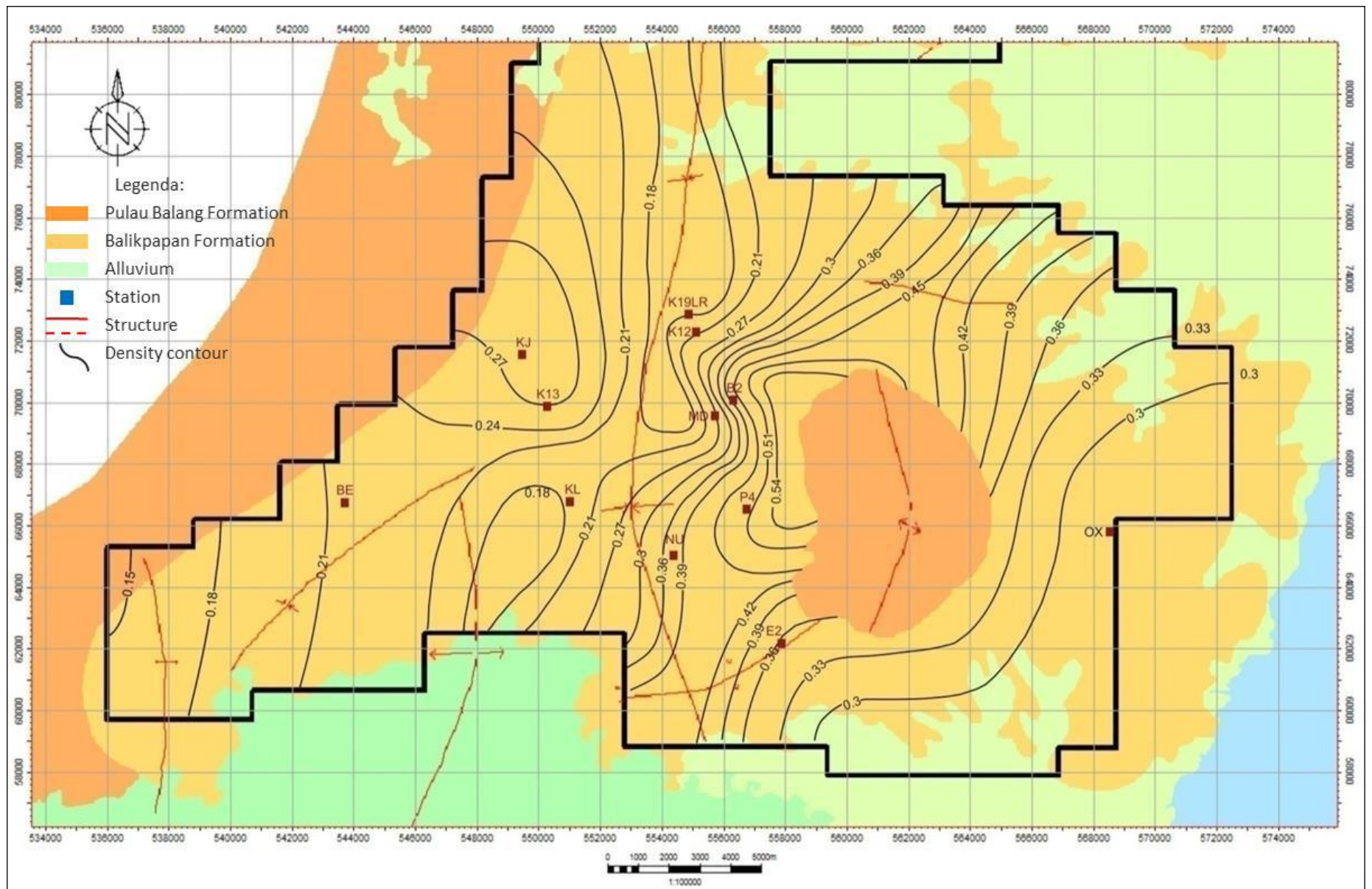
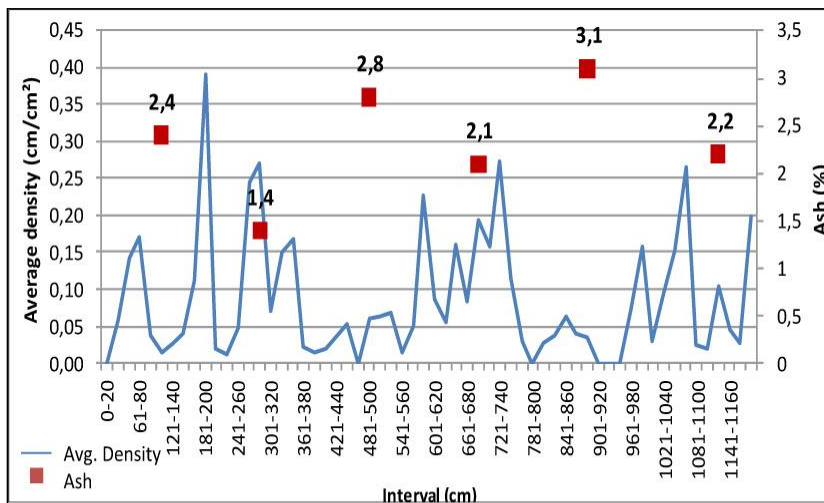
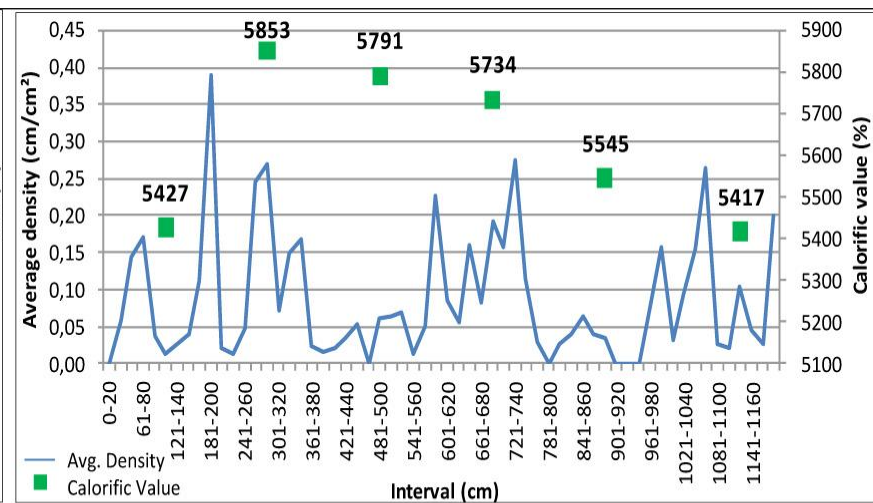


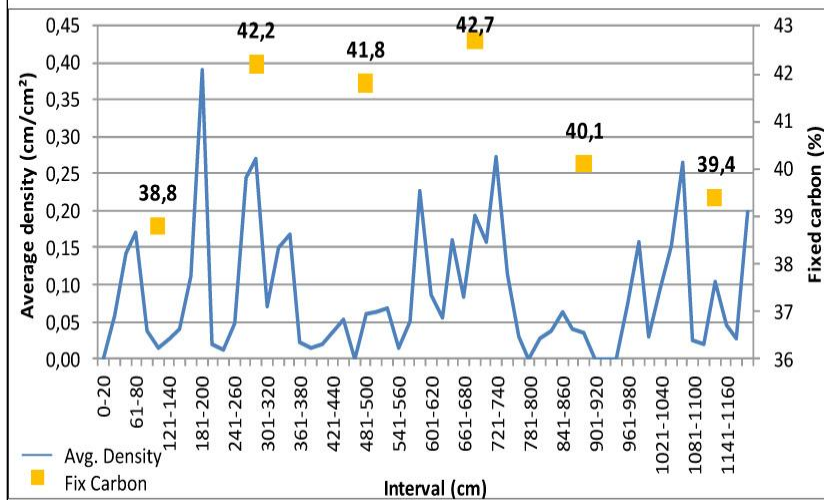
Figure 11. Cleat density map.



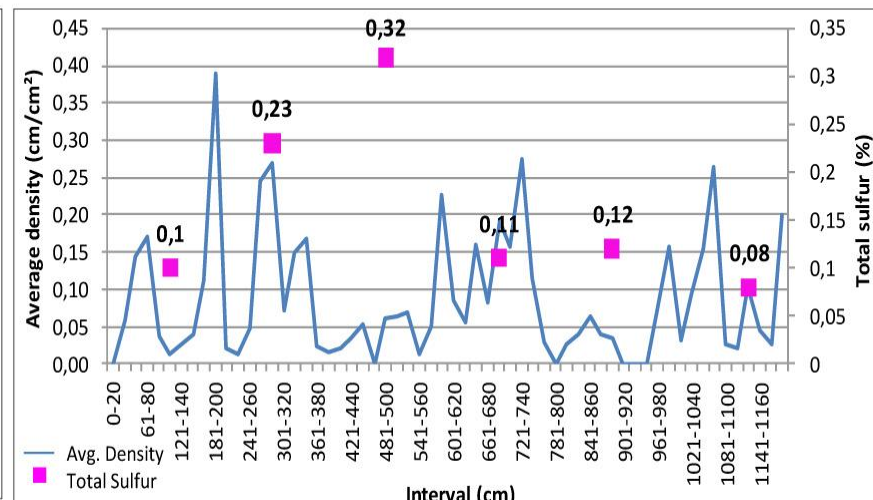
(a) Avg. Density and Ash



(b) Avg. Density and Calorific value



(c) Avg. Density and Fix carbon



(d) Avg. Density and Total Sulfur

Figure 12. Average density and coal quality.

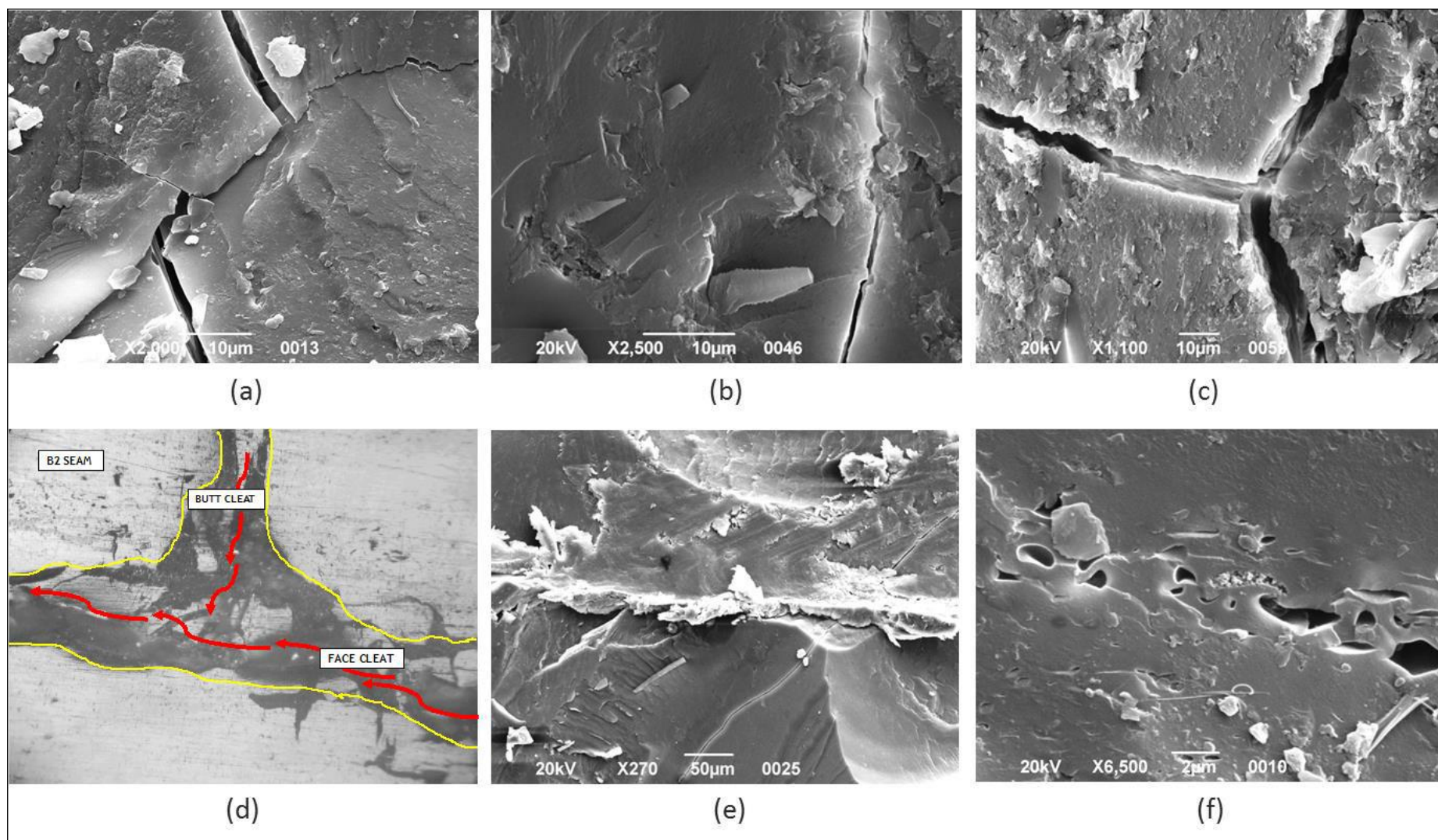


Figure 13. (a, b, c, d) Micro-cleats, (e) cleat filled by mineral, (f) agglutination.

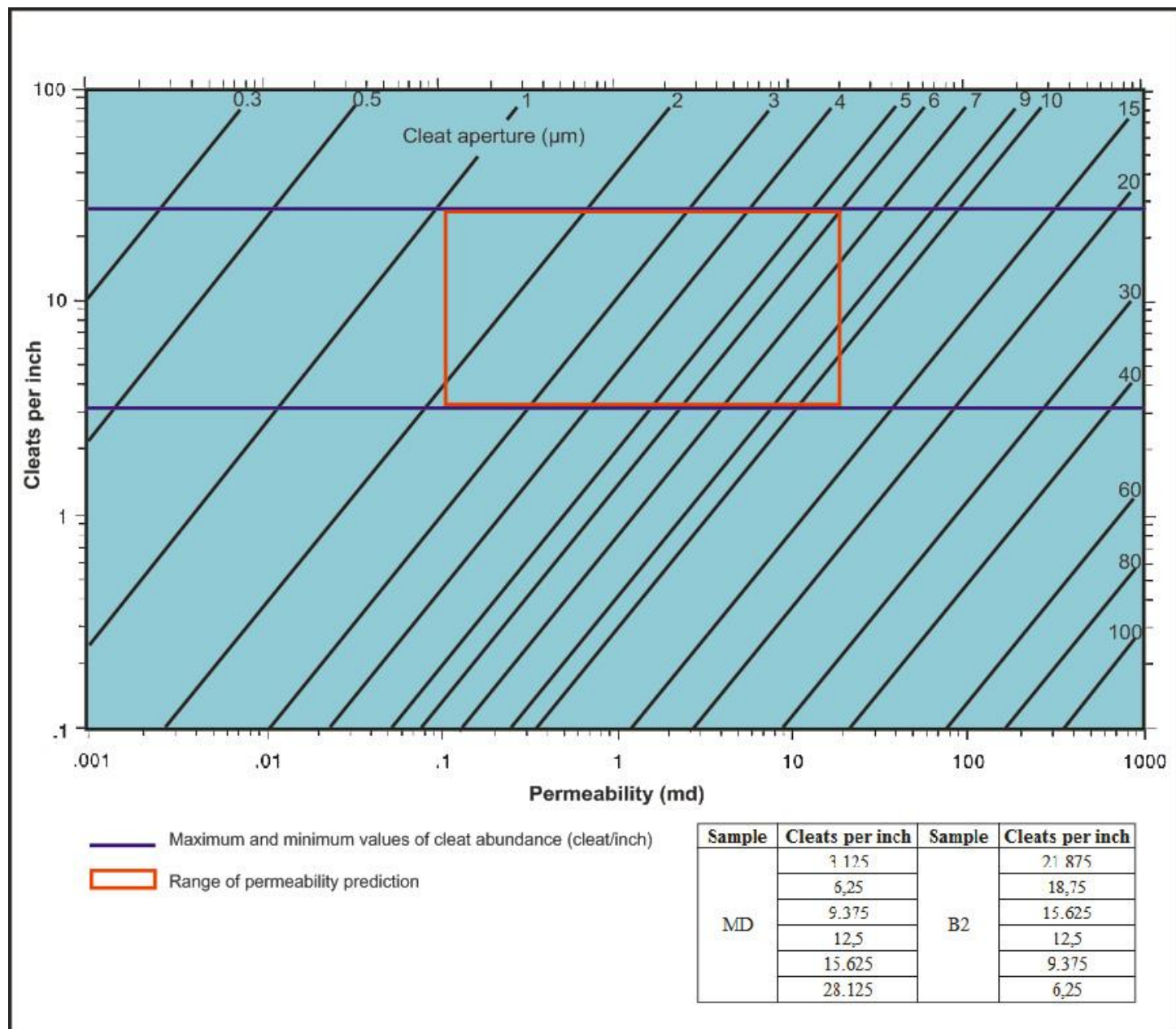
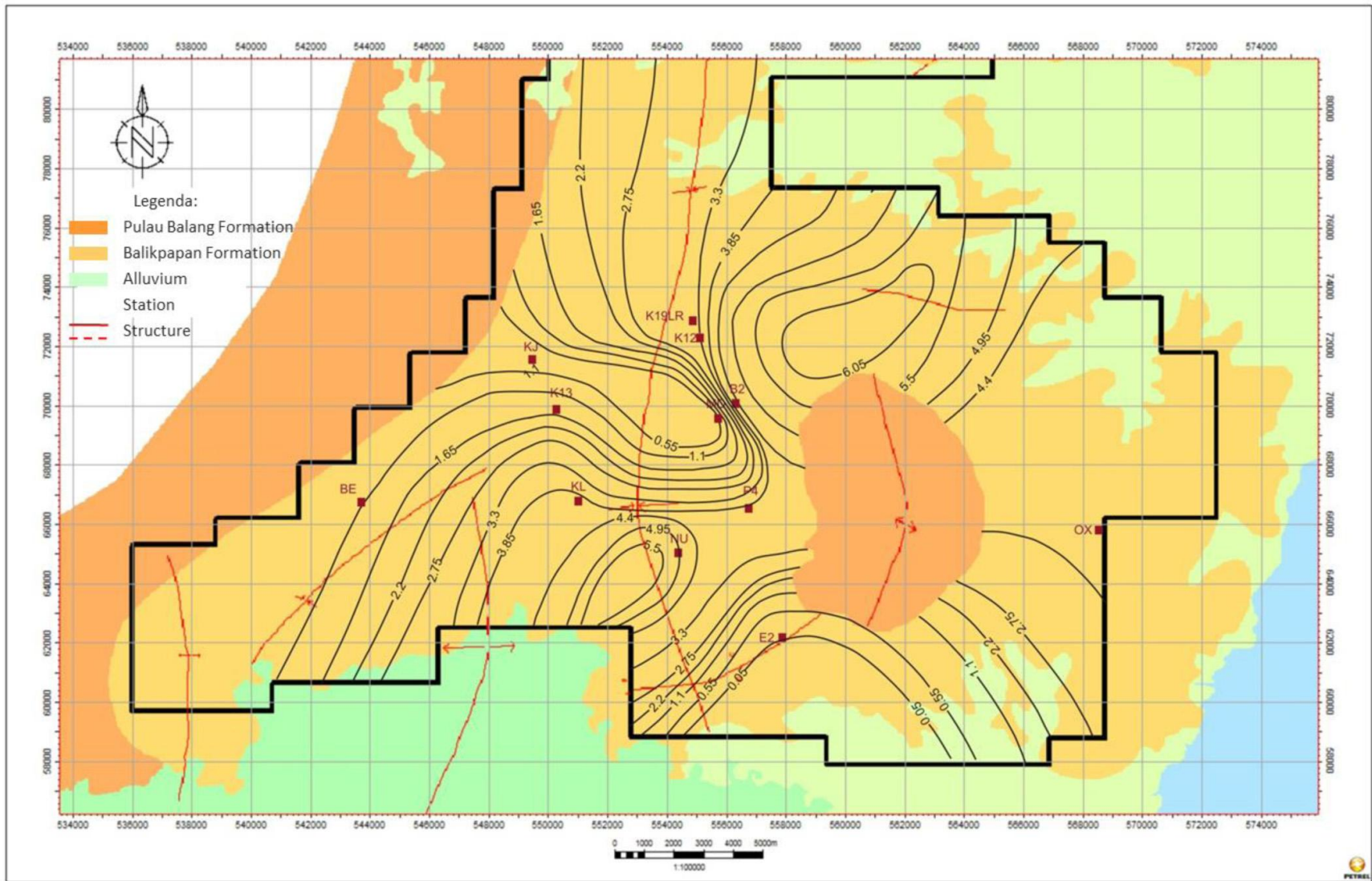


Figure 14. Average density and coal quality.



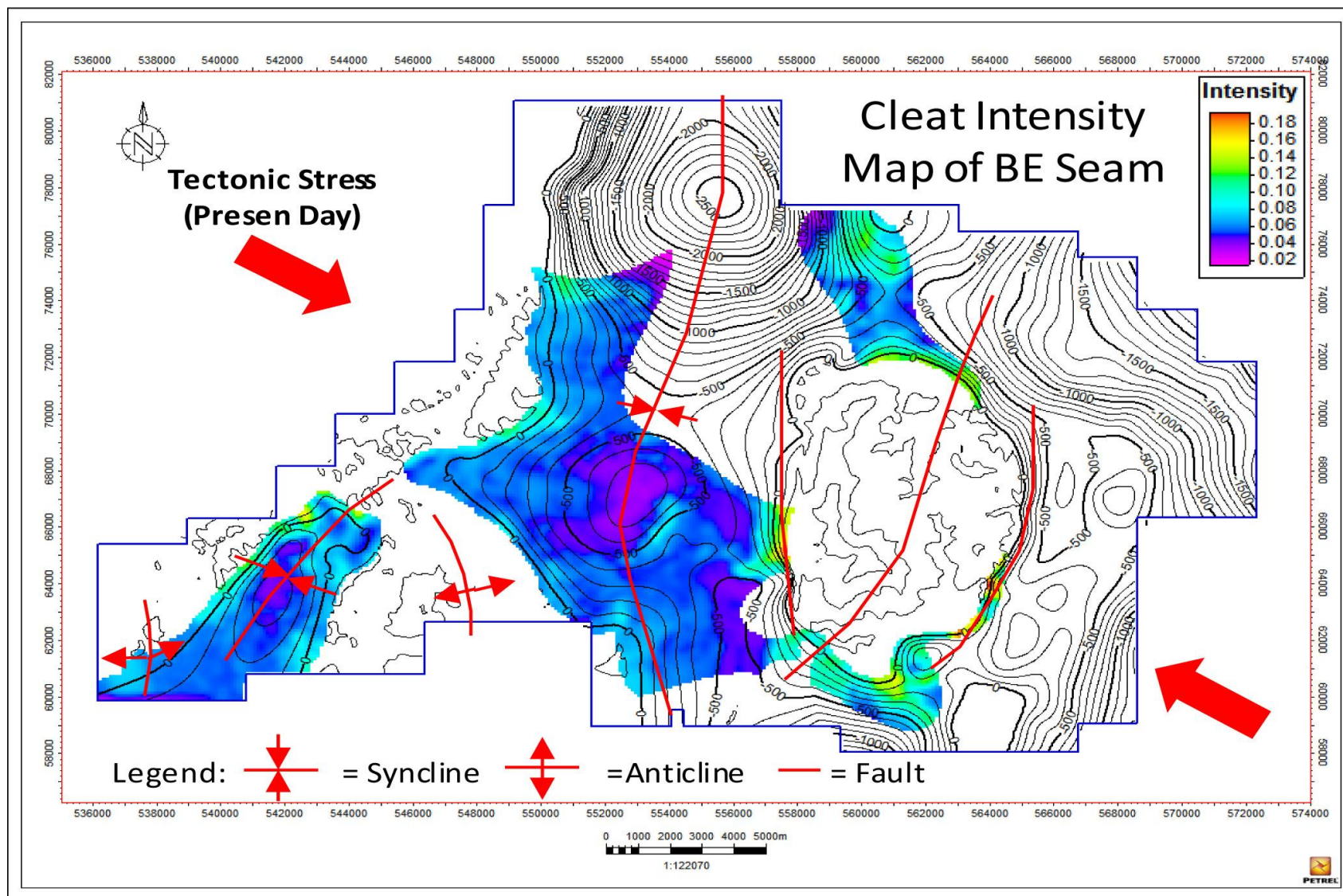


Figure 16. Cleat intensity model.

STATION	UTM		Spacing		Aperture	
	X	Y	y	R ²	y	R ²
K19LR	554898	72885	$170.2x^{-1.35}$	0.951	$2.010x^{-0.79}$	0.978
B2	556287	70093	$10409x^{-3.56}$	0.97	$0.016x^{-2.55}$	0.957
NU	554348	64997	$0997.5x^{-2.69}$	0.975	$0.053x^{-2.33}$	0.979
P4	556770	66544	$448.9x^{-2.42}$	0.983	$0.002x^{-3.68}$	0.96
OX	568801	65801	$384.5x^{-1.65}$	0.95	$0.006x^{-3.11}$	0.936
KL	551010	66763	$3309.x^{-2.93}$	0.96	$0.052x^{-2.23}$	0.949
BE	543689	66725	$4979.x^{-2.27}$	0.974	$0.058x^{-2.44}$	0.966
K13	550267	69871	$1328.x^{-2.31}$	0.966	$0.012x^{-3.16}$	0.951
KJ	549459	71589	$501.9x^{-2.02}$	0.972	$187.4x^{-0.10}$	0.916
E	565427	92182	$994.3x^{-1.85}$	0.975	$0.000x^{-3.99}$	0.934
A	558000	89324	$1078.x^{-2.84}$	0.973	$0.142x^{-1.65}$	0.943
K12	555089	72235	$922.3x^{-2.05}$	0.951	$0.232x^{-2.03}$	0.948
E2	557873	62145	$195.1x^{-1.54}$	0.959		

Table 1. Cleat measurement.

Stasion	UTM		Formation	Area (cm ²)	Intensity	Average density (cm/cm ²)	Average aperture (cm)	Average height (cm)
	X	Y						
K19LR	554898	72885	Balikpapan	10000	125	0,171	0,054	13,677
B2	556287	70093	Balikpapan	10000	489	0,473	0,029	10,889
MD	555743	69547	Balikpapan	10000	63	0,247	0,018	39,143
NU	554348	64997	Balikpapan	10000	43	0,377	0,021	87,558
P4	556770	66544	Balikpapan	10000	153	0,506	0,039	33,052
OX	568801	65801	Balikpapan	10000	97	0,294	0,056	30,258
KL	551010	66763	Balikpapan	10000	98	0,183	0,044	18,714
BE	543689	66725	Balikpapan	10000	138	0,214	0,020	15,522
K13	550267	69871	Balikpapan	10000	139	0,270	0,038	19,446
E	565427	92182	Balikpapan	10000	133	0,191	0,034	14,346
A	558000	89324	Balikpapan	10000	193	0,418	0,025	21,632
K12	555089	72235	Balikpapan	10000	113	0,205	0,040	18,106
E2	557873	62145	Balikpapan	10000	194	0,328	0,020	16,907

Table 2. Quantitative analysis based on scanline data.

Station	Total Height		Density		Cumulative Height	Area (cm2)	Cleat Density
	Face	Butt	Face	Butt			
K19LR	1478	231,6	0,1478	0,02316	1709,6	10000	0,171
B2	3316	1410	0,3316	0,141	4726	10000	0,473
MD	2466	0	0,2466	0	2466	10000	0,247
NU	3765	0	0,3765	0	3765	10000	0,377
P4	5014	43	0,5014	0,0043	5057	10000	0,506
OX	2935	0	0,2935	0	2935	10000	0,294
KL	1834	0	0,1834	0	1834	10000	0,183
BE	1620	522	0,162	0,0522	2142	10000	0,214
K13	2703	0	0,2703	0	2703	10000	0,270
KJ	2797	0	0,3756	0,2797	2797	10000	0,280
E	1908	0	0,1908	0	1908	10000	0,191
A	3466	709	0,3466	0,0709	4175	10000	0,418
K12	2046	0	0,2046	0	2046	10000	0,205
E2	2219	1261	0,2219	0,1261	3480	10000	0,348

Table 3. Quantitative analysis based on window scan data.

STATION	UTM		Spacing		Aperture	
	X	Y	y	R ²	y	R ²
K19LR	554898	72885	$170.2x^{-1.35}$	0.951	$2.010x^{-0.79}$	0.978
B2	556287	70093	$10409x^{-3.56}$	0.97	$0.016x^{-2.55}$	0.957
NU	554348	64997	$0997.5x^{-2.69}$	0.975	$0.053x^{-2.33}$	0.979
P4	556770	66544	$448.9x^{-2.42}$	0.983	$0.002x^{-3.68}$	0.96
OX	568801	65801	$384.5x^{-1.65}$	0.95	$0.006x^{-3.11}$	0.936
KL	551010	66763	$3309.x^{-2.93}$	0.96	$0.052x^{-2.23}$	0.949
BE	543689	66725	$4979.x^{-2.27}$	0.974	$0.058x^{-2.44}$	0.966
K13	550267	69871	$1328.x^{-2.31}$	0.966	$0.012x^{-3.16}$	0.951
KJ	549459	71589	$501.9x^{-2.02}$	0.972	$187.4x^{-0.10}$	0.916
E	565427	92182	$994.3x^{-1.85}$	0.975	$0.000x^{-3.99}$	0.934
A	558000	89324	$1078.x^{-2.84}$	0.973	$0.142x^{-1.65}$	0.943
K12	555089	72235	$922.3x^{-2.05}$	0.951	$0.232x^{-2.03}$	0.948
E2	557873	62145	$195.1x^{-1.54}$	0.959		

Table 4. A power-law distribution exists between cumulative fracture with spacing and aperture r-square values greater than 0.93.

Station	Total Height		Density		Cumulative Height	Area (cm2)	Cleat Density
	Face	Butt	Face	Butt			
K19LR	1478	231,6	0,1478	0,02316	1709,6	10000	0,171
B2	3316	1410	0,3316	0,141	4726	10000	0,473
MD	2466	0	0,2466	0	2466	10000	0,247
NU	3765	0	0,3765	0	3765	10000	0,377
P4	5014	43	0,5014	0,0043	5057	10000	0,506
OX	2935	0	0,2935	0	2935	10000	0,294
KL	1834	0	0,1834	0	1834	10000	0,183
BE	1620	522	0,162	0,0522	2142	10000	0,214
K13	2703	0	0,2703	0	2703	10000	0,270
KJ	2797	0	0,3756	0,2797	2797	10000	0,280
E	1908	0	0,1908	0	1908	10000	0,191
A	3466	709	0,3466	0,0709	4175	10000	0,418
K12	2046	0	0,2046	0	2046	10000	0,205
E2	2219	1261	0,2219	0,1261	3480	10000	0,348

Table 5. The cleat density for individual seams varies between 0.17cm/ cm2– 0.51 cm/cm2

Station	PROXIMATE ANALYSIS							
	Total Moisture	Inherent Moisture	Ash	Volatile Matter	Fixed Carbon	Relative Density	Calorific Value	Total Sulphur
	TM (%)	IM%	%	VM%	FC%	RD%	CV (kcal/kg)	TS%
K19LR	25,10	19,20	3,50	37,30	40,00	1,27	5623,00	0,31
B2	19,54	12,09	3,20	39,10	45,61	1,31	6306,94	0,82
SU	11,95	9,00	5,80	39,15	46,05	1,33	6530,00	2,64
MD	15,97	11,10	3,07	40,06	46,44	1,30	6577,30	0,32
NU	17,55	13,69	3,83	37,53	44,96	1,31	6196,25	0,81
P4	19,32	15,47	2,57	37,31	44,65	1,30	6053,60	0,63
KL	19,10	15,45	7,65	35,30	41,60	1,34	5585,00	0,76
BE	23,36	18,04	2,12	38,76	41,08	1,30	5672,41	0,14
K13	32,77	24,55	3,83	35,80	35,82	1,32	5005,50	0,46
E	16,12	11,72	2,68	39,42	46,18	1,32	6462,65	1,09
A	18,47	14,67	8,06	37,17	40,39	1,35	5809,57	0,54
K12	22,85	18,20	4,95	37,30	39,55	1,28	5586,50	0,27
E2	9,60	6,94	10,95	36,20	45,90	1,34	6342,00	1,85

Table 6. Coal quality analysis.

Station	Average Aperture (cm)	Average Spacing (cm)	Cleat Permeability (darcys)	
			Cubes	Match Sticks
K19LR	0,050	9,002	3,938	2,95
B2	0,044	3,707	5,677	4,26
MD	0,022	5,057	0,261	0,20
NU	0,040	2,148	6,679	5,01
P4	0,035	1,626	5,124	3,84
OX	0,044	4,364	4,750	3,56
KL	0,045	4,354	5,105	3,83
BE	0,036	6,841	1,357	1,02
K13	0,053	21,596	1,991	1,49
E	0,033	3,056	2,116	1,59
A	0,035	2,106	3,779	2,83
K12	0,071	5,346	4,280	3,21
E2	0,015	4,745	0,062	0,05

Table 7. Coal quality analysis.